

# Neutral Hydrogen Gas in Interacting Galaxies: The NGC 1511 galaxy group<sup>★</sup>

Bärbel Koribalski<sup>1</sup> and Eva Manthey<sup>2</sup>

<sup>1</sup>*Australia Telescope National Facility, CSIRO, P.O. Box 76, Epping, NSW 1710, Australia*

<sup>2</sup>*University of Bochum, Department of Astronomy, 44780 Bochum, Germany*

Received date; accepted date

## ABSTRACT

We present H I line and 20-cm radio continuum observations of the NGC 1511 galaxy group obtained with the Australia Telescope Compact Array. The data reveal an extended, rather disturbed H I distribution for the peculiar starburst galaxy NGC 1511 and a narrow bridge to its small companion galaxy, NGC 1511B, which has been severely distorted by the interaction/collision between the two galaxies. No stellar counterpart to the gaseous bridge has been detected. In addition, we find that the peculiar optical ridge to the east of NGC 1511 is probably the stellar remnant of a galaxy completed disrupted by interactions with NGC 1511. The slightly more distant neighbour, NGC 1511A, shows a regular H I velocity field and no obvious signs of interactions.

Radio continuum emission from NGC 1511 reveals three prominent sources on top of a more diffuse, extended distribution. We derive an overall star formation rate of  $7 M_{\odot} \text{yr}^{-1}$ . The most enhanced star formation is found in the south-eastern part of the disk, coincident with several bright H II regions, and closest to the peculiar optical ridge. No continuum emission was detected in the companions, but NGC 1511B appears to show an H II region at its faint western edge, closest to NGC 1511. The group displays a prime example of interaction-induced star formation activity.

**Key words:** galaxies: individual (NGC 1511, NGC 1511A, NGC 1511B) — galaxies: interacting

## 1 INTRODUCTION

Neutral hydrogen gas (H I) is the best tracer for galaxy-galaxy interactions. Since the H I envelope of a galaxy is generally more extended than its stellar disk (Broeils & van Woerden 1994; Salpeter & Hoffman 1996) it is more easily disrupted by tidal forces from neighboring galaxies. Galaxy pairs and groups often show very complex extended H I distributions, incl. H I tails and bridges, even if the corresponding optical images show little disturbance. For examples see Irwin (1994), Smith, Struck & Pogge (1997), Yun et al. (1994), Koribalski & Dickey (2004), and the H I Rogues Gallery (Hibbard et al. 2001). Here we use H I line observations to investigate the interaction history and dynamics of the NGC 1511 galaxy group.

The starburst galaxy NGC 1511 is the most prominent member of a compact galaxy triplet at a distance of  $\sim 17.5$  Mpc ( $H_0 = 75 \text{ km s}^{-1} \text{ Mpc}^{-1}$ ). Its companions, NGC 1511B

and NGC 1511A, lie at projected distances of  $7'.3$  (37 kpc) and  $10'.7$  (54 kpc), respectively. Table 1 lists some properties for all three galaxies. The stellar disk of NGC 1511 (see, e.g., Eskridge et al. 2000, Sandage & Bedke 1994) contains several bright hotspots, a prominent dust lane and various peculiar extensions. Faint loops and plumes are seen to the northeast of the disk while the hotspots are located in a peculiar hook at the south-eastern end of the disk which is best seen in infrared images (Eskridge et al. 2000, Jarret et al. 2003). In addition, deep optical images reveal an extended vertical ridge  $\sim 1'.5$  east of the south-eastern end of the disk, the nature of which we will explore here. Optical short exposures of NGC 1511 show a remarkable resemblance to the peculiar starburst galaxy NGC 1808 (Koribalski et al. 1993). The optical diameter of NGC 1511 ( $3'.5 \times 1'.2$  or  $17.5 \text{ kpc} \times 6.1 \text{ kpc}$ ) is about twice that of the neighboring galaxies NGC 1511A and B. While NGC 1511A appears slightly inclined and symmetric, NGC 1511B is an extremely thin, edge-on galaxy with a faint extension to the west. There is a hint of an H II region at the western most end. The peculiarities of both NGC 1511 and NGC 1511B suggest they are interacting. Koribalski (1996) briefly commented on the

<sup>★</sup> The observations were obtained with the Australia Telescope which is funded by the Commonwealth of Australia for operations as a National Facility managed by CSIRO.

post interaction/merger nature of NGC 1511. The H I distribution of the triplet is also briefly discussed by Nordgren et al. (1997). The star formation history of NGC 1511 can be used to estimate the interaction time scale. Sekiguchi & Wolstencroft (1993) find that NGC 1511 has an H II region like emission spectrum with high excitation (see also Kewley et al. 2000), suggesting on-going star formation mixed with a burst  $\sim 10^8 - 10^9$  yrs ago. Thornley et al. (2000) find indications of massive star formation ( $\gtrsim 50 M_{\odot}$ ) on a short timescale of  $\leq 10^7$  yr using mid-infrared spectroscopy. Elfhag et al. (1996) observed the center of NGC 1511 with the SEST and find a CO intensity of  $I_{\text{CO}} = 11.5 \text{ K km s}^{-1}$  (adjusted to our adopted distance). This corresponds to a nuclear H<sub>2</sub> mass of  $5.5 \times 10^8 M_{\odot}$  if we adopt the standard conversion factor of  $N_{\text{H}_2}/I_{\text{CO}} = 2.3 \times 10^{20} \text{ H}_2 \text{ cm}^{-2} (\text{K km s}^{-1})^{-1}$  (Strong et al. 1988). Radio continuum, X-ray, and UV data were obtained by Dahlem et al. (2001, 2003), while Lehnert & Heckman (1995) presented an H $\alpha$  image. These data confirm the starburst character of NGC 1511.

The paper is organized as follows: in Section 2 we summarize the observations and data reduction. In Section 3 we present the 20-cm radio continuum results and derive star formation rates for NGC 1511. The H I morphology and kinematics of all members of the NGC 1511 galaxy group are described in Section 4. The overall gas dynamics are discussed in Section 5, and Section 6 contains our conclusions.

## 2 OBSERVATIONS AND DATA REDUCTION

H I line and 20-cm radio continuum observations of the NGC 1511 galaxy group were obtained with the Australia Telescope Compact Array (ATCA) in March and August 1995 using the 1.5A and 375 arrays. For a summary of the observations see Table 2.

Data reduction was carried out with the MIRIAD software package using standard procedures. The data were split into a narrow band radio continuum and an H I line data set using a first order fit to the line-free channels. The H I channel maps were made using ‘natural’ (na) and ‘robust’ (r=0) weighting of the  $uv$ -data in the velocity range from 1050 to 1550  $\text{km s}^{-1}$  using steps of 10  $\text{km s}^{-1}$ . The resulting synthesized beams are  $64'' \times 63''$  (na) and  $31.8'' \times 31.2''$  (r=0); the measured r.m.s. noise is 1.7 and 1.8  $\text{mJy beam}^{-1}$ , respectively. The H I data cubes were corrected for primary beam attenuation. One  $\text{Jy beam}^{-1} \text{ km s}^{-1}$  corresponds to an H I column density of  $2.8 \times 10^{20} \text{ atoms cm}^{-2}$  (na) and  $11.2 \times 10^{20} \text{ atoms cm}^{-2}$  (r=0).

Radio continuum maps were made using ‘uniform’ weighting of the  $uv$ -data. After CLEANing they were restored with a synthesized beam of  $6''$ , resulting in an r.m.s. of  $0.5 \text{ mJy beam}^{-1}$ . A low-resolution image was created using ‘natural weighting’; only the shortest 10 baselines were used. The beam size here is  $76'' \times 71''$ , with an r.m.s. of  $0.8 \text{ mJy beam}^{-1}$ .

## 3 RADIO CONTINUUM RESULTS

Since the overall, extended radio continuum emission of NGC 1511 was analysed by Dahlem et al. (2001), we concentrate here on the central region. Fig. 1 shows a high-

**Table 2.** Observing parameters.

ATCA configuration	1.5A	375
primary beam	33'	
pointing position	03 <sup>h</sup> 59 <sup>m</sup> 25 <sup>s</sup>	
in $\alpha, \delta(\text{J2000})$	−67° 47' 00''	
total observing time	712 min.	647 min.
center frequency	1414 MHz	
total bandwidth	8 MHz	
number of channels	512	
velocity resolution	6.6 $\text{km s}^{-1}$	
(after Hanning smoothing)		
Calibrator flux densities:		
primary	1934–638 (14.88 Jy)	
secondary	0355–669 (0.97 Jy)	

resolution 20-cm radio continuum image of NGC 1511 overlaid onto B- and H-band images from Eskridge et al. (2000). We identify three maxima in  $\alpha, \delta(\text{J2000}) = 03^{\text{h}} 59^{\text{m}} 40^{\text{s}}.7, -67^{\circ} 38' 23''.8$  (SE complex),  $03^{\text{h}} 59^{\text{m}} 36^{\text{s}}.5, -67^{\circ} 38' 02''.0$  (middle source) and  $03^{\text{h}} 59^{\text{m}} 33^{\text{s}}.7, -67^{\circ} 38' 01''.1$  (faint western source) with approximate peak flux densities of 53, 27 and 13  $\text{mJy beam}^{-1}$ , respectively. The SE complex corresponds to the peculiar hook which is best seen in the H-band image (Eskridge et al. 2000) and the 2MASS JHKs-image (Jarret et al. 2003). At the same location, the B-band image shows a chain of bright hotspots. These are young H II regions (see Lehnert & Heckman 1995) consistent with increased star formation in that part of the disk of NGC 1511. The middle source, which lies  $\sim 6''$  northeast of the galaxy center as given in Table 1, and the faint western source also appear to coincide with hotspots in the H $\alpha$  image. No radio continuum emission was detected from the companions, NGC 1511A and NGC 1511B, with  $5\sigma$  upper limits to their flux densities of  $\sim 4 \text{ mJy}$ . We detect several background sources in the observed field; the two brightest are SUMSS J035734–674941 (30 mJy) and SUMSS J035949–680052 (68 mJy).

To estimate the star formation rate (SFR) of NGC 1511 from the 20-cm radio continuum flux density,  $S_{20}$  (Jy), we use  $\text{SFR} (M_{\odot} \text{ yr}^{-1}) = 0.14 D^2 S_{20 \text{ cm}}$  derived from Condon (1992) and Haarsma et al. (2000), where  $D$  is the distance in Mpc. For NGC 1511 we measure a primary beam corrected 20-cm radio continuum flux density of 167 mJy (using the low-resolution map) and hence a star formation rate of  $\sim 7 M_{\odot} \text{ yr}^{-1}$ . There are indications of a faint extended halo, but our data are not sufficient to study this emission. For comparison, Dahlem et al. (2001) measure a total 20-cm radio continuum flux density of  $156 \pm 8 \text{ mJy}$ . For NGC 1511A and B we derive upper limits of  $\text{SFR} < 0.2 M_{\odot} \text{ yr}^{-1}$ .

The star formation rate of a galaxy can also be estimated from its far-infrared luminosity,  $L_{\text{FIR}}$ , using  $\text{SFR} (M_{\odot} \text{ yr}^{-1}) = 0.17 L_{\text{FIR}}$  (Kennicutt 1998), with  $L_{\text{FIR}}$  in units of  $10^9 L_{\odot}$ . Using the IRAS 60 $\mu\text{m}$  and 100 $\mu\text{m}$  flux densities given by Sanders et al. (1995) ( $S_{60\mu\text{m}} = 25.7 \text{ Jy}$ ,  $S_{100\mu\text{m}} = 41.3 \text{ Jy}$ , for comparison see Table 1) we derive a FIR luminosity of  $1.36 \times 10^{10} L_{\odot}$  for NGC 1511 which results in  $\text{SFR} = 2.2 M_{\odot} \text{ yr}^{-1}$ . NGC 1511A has an infrared luminosity of  $1.4 - 4.0 \times 10^8 L_{\odot}$  and  $\text{SFR} = 0.02 - 0.07 M_{\odot} \text{ yr}^{-1}$ . No IRAS flux densities are available for NGC 1511B.

Following Helou, Soifer & Rowan-Robinson (1985) we calculated the parameter  $q$  which is the logarithmic ratio

**Table 1.** Some basic parameters of the observed spiral galaxies.

	NGC 1511	NGC 1511A	NGC 1511B	Ref.
center position:				
$\alpha$ (J2000)	03 <sup>h</sup> 59 <sup>m</sup> 35 <sup>s</sup> .8	04 <sup>h</sup> 00 <sup>m</sup> 19 <sup>s</sup> .4	04 <sup>h</sup> 00 <sup>m</sup> 54 <sup>s</sup> .6	(1)
$\delta$ (J2000)	-67°38'07"	-67°48'28"	-67°36'42"	
type	SAa pec	SB0	SBd?	(1)
optical diameter	3.5 × 1.2	1.7 × 0.4	1.7 × 0.3	(1)
inclination	74 ± 2	75 ± 4	87 ± 4	(6)
position angle	125°	110°	98°	(1,2)
$v_{\text{HI}}$ [km s <sup>-1</sup> ]	1351 ± 7	1323 ± 10	1304 ± 3	(1,3,6)
$v_{\text{opt}}$ [km s <sup>-1</sup> ]	1334 ± 48	1358 ± 69	—	(1)
$v_{\text{H}\alpha}$ [km s <sup>-1</sup> ]	1334 ± 10	1291 ± 10	1439 ± 10	(2)
$v_{\text{CO}}$ [km s <sup>-1</sup> ]	1270 ± 7	—	—	(4)
$F_{\text{HI}}$ [Jy km s <sup>-1</sup> ]	73.6	20.6	—	(3)
S <sub>60<math>\mu</math>m</sub> [Jy]	23.67	0.44	—	(5)
S <sub>100<math>\mu</math>m</sub> [Jy]	37.99	<2.16	—	(5)
B magnitude	12.11	14.23	15.12	(1)
A <sub>B</sub>	0.265	0.257	0.236	(7)
$L_{\text{B}}$ [10 <sup>9</sup> L <sub>⊙</sub> ]	4.9	0.7	0.3	
$L_{\text{X}}$ [10 <sup>40</sup> erg s <sup>-1</sup> ]	1.1	—	—	(8)

References: (1) de Vaucouleurs et al. 1991 [RC3], (2) Lauberts 1982 [ESO-LV], (3) Mathewson & Ford 1996, (4) Elfhag et al. 1996, (5) Moshir et al. 1990, (6) Nordgren et al. 1997, (7) Schlegel et al. 1998, (8) Dahlem et al. 2003.

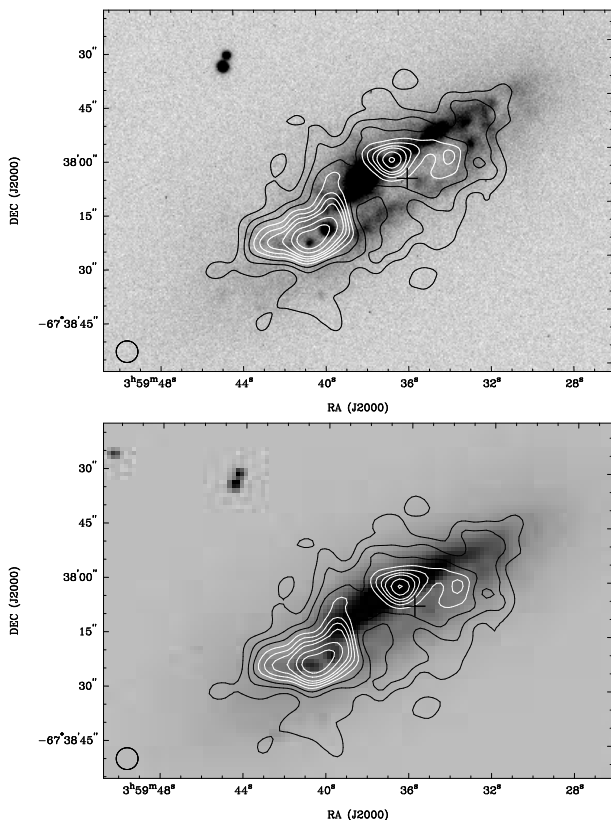


**Figure 1.** High-resolution 20-cm radio continuum emission of NGC 1511 overlaid onto B-band (top) and H-band (bottom) images from Eskridge et al. (2000). The contour levels are 1, 1.5, 2, 2.5, 3, 3.5, 4, 4.5, 5, 5.5, 6, and 6.5 mJy beam<sup>-1</sup>. The galaxy center (see Table 1) is marked with a cross. The synthesized beam (6'') is displayed at the bottom left corner.

of FIR to radio flux density. For NGC 1511 we find  $q = 2.34$ , consistent with the mean value of 2.3 for normal spiral galaxies (Condon 1992).

#### 4 H I RESULTS

The H I channel maps of the NGC 1511 group are shown in Fig. 2. All three galaxies are clearly detected, covering a velocity range of 1130 to 1510 km s<sup>-1</sup>. In addition, we detect a thin H I bridge between NGC 1511 and NGC 1511B, indicating tidal interactions or a direct collision of the two galaxies. No bridge is detected towards NGC 1511A. The individual H I spectra are displayed in Fig. 3. Most noticeable is the rather narrow H I spectrum (1370 – 1480 km s<sup>-1</sup>) of the disturbed, edge-on galaxy NGC 1511B, in contrast to the broad spectra of NGC 1511 and NGC 1511A. We estimate the systemic velocity of NGC 1511B to be 1425 km s<sup>-1</sup>, close to the H $\alpha$  velocity (see Table 1). Note that Nordgren et al. (1997) find the H I spectrum of NGC 1511B peaks at 1429 km s<sup>-1</sup>, in agreement with our value. Because they claim to see faint H I emission at lower velocities, they estimate  $v_{\text{sys}} = 1304$  km s<sup>-1</sup>. The H I bridge, which appears to connect the north-western edge of NGC 1511 to the western edge of NGC 1511B covers a velocity range from  $\sim 1320$  to 1430 km s<sup>-1</sup>. Both the H I and the stellar disk of NGC 1511B are affected by the interaction. It is likely that the gas in the H I bridge was stripped from NGC 1511B by a direct collision with the outer disk of NGC 1511.

The H I distribution, the mean H I velocity field and the H I velocity dispersion of the NGC 1511 group are shown in Fig. 4. For a summary of the H I properties see Table 3.

We measure a total primary-beam corrected H I flux density of  $F_{\text{HI}} = 74$  Jy km s<sup>-1</sup> for the NGC 1511 group resulting in an H I mass of  $M_{\text{HI}} = 5.4 \times 10^9 M_{\odot}$ . For NGC 1511 alone we measure  $F_{\text{HI}} = 66.4$  Jy km s<sup>-1</sup> which corresponds to an H I mass of  $4.8 \times 10^9 M_{\odot}$ , while the two small companions, NGC 1511A and NGC 1511B, have H I masses of 2.0

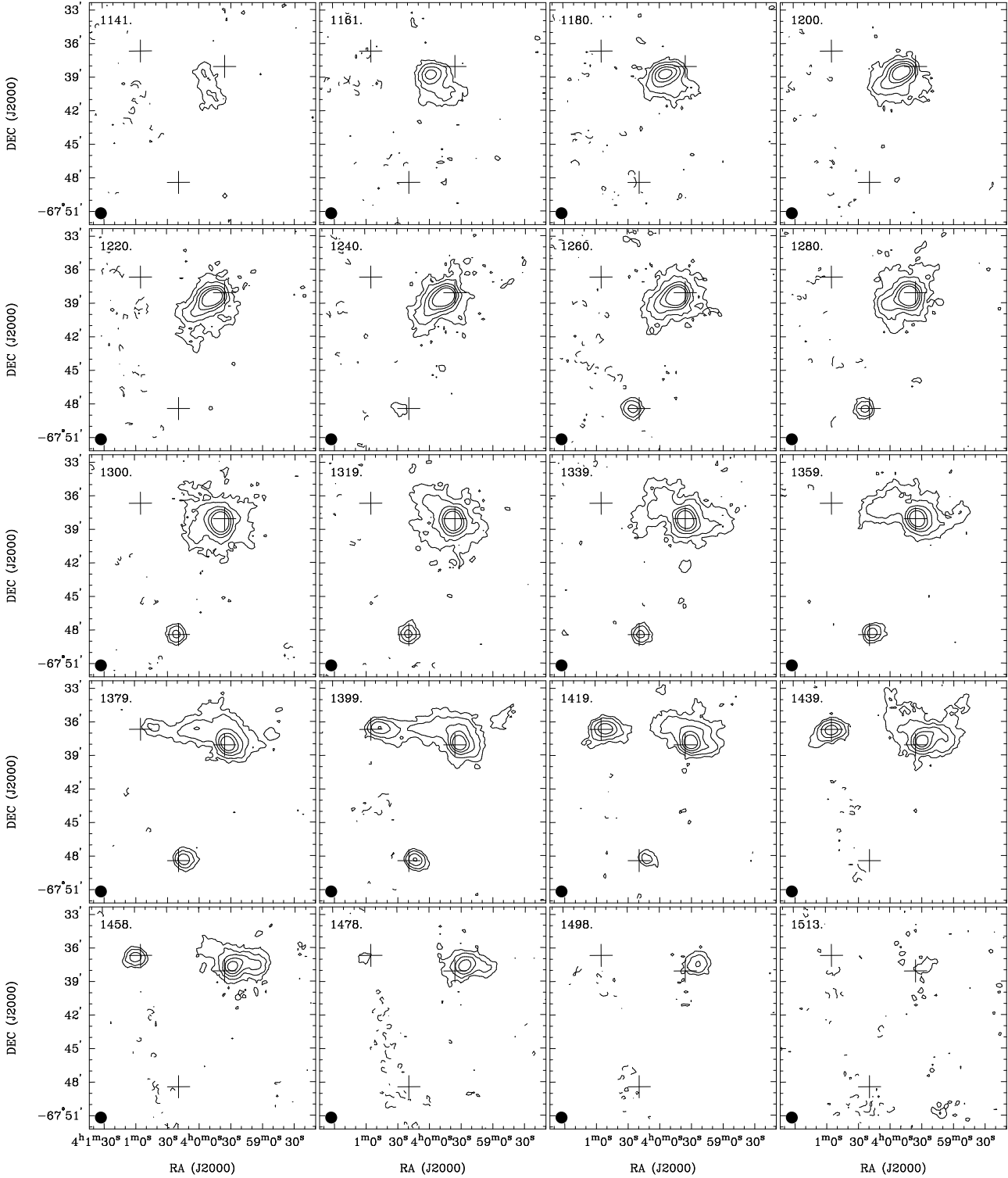


**Figure 2.** HI channel maps of the NGC 1511 group using ‘natural’ weighting. The three galaxy centers are marked as given in Table 1. The contour levels are  $-3, 3, 6, 12, 20,$  and  $30 \text{ mJy beam}^{-1}$ . The synthesized beam ( $64'' \times 63''$ ) is displayed at the bottom left corner and the heliocentric velocity of each channel at the top left.

and  $3.7 \times 10^8 M_{\odot}$ , respectively. For a summary see Table 3. The HIPASS Bright Galaxy Catalog (Koribalski et al. 2004) gives the following HI properties for NGC 1511 (HIPASS J0359–67): a systemic velocity of  $v_{\text{sys}} = 1333 \pm 5 \text{ km s}^{-1}$ , 50% and 20% velocity widths of  $267 \text{ km s}^{-1}$  and  $323 \text{ km s}^{-1}$ ,

respectively, and  $F_{\text{HI}} = 65.9 \pm 5.0 \text{ Jy km s}^{-1}$ , i.e.  $M_{\text{HI}} = 4.8 (\pm 0.3) \times 10^9 M_{\odot}$ . The HI flux density given in HICAT ( $F_{\text{HI}} = 74.2 \text{ km s}^{-1}$ , Meyer et al. 2004) was measured over a larger area ( $36' \times 36'$ ) and is consistent with our HI measurement of the whole group. This agreement indicates that very lit-

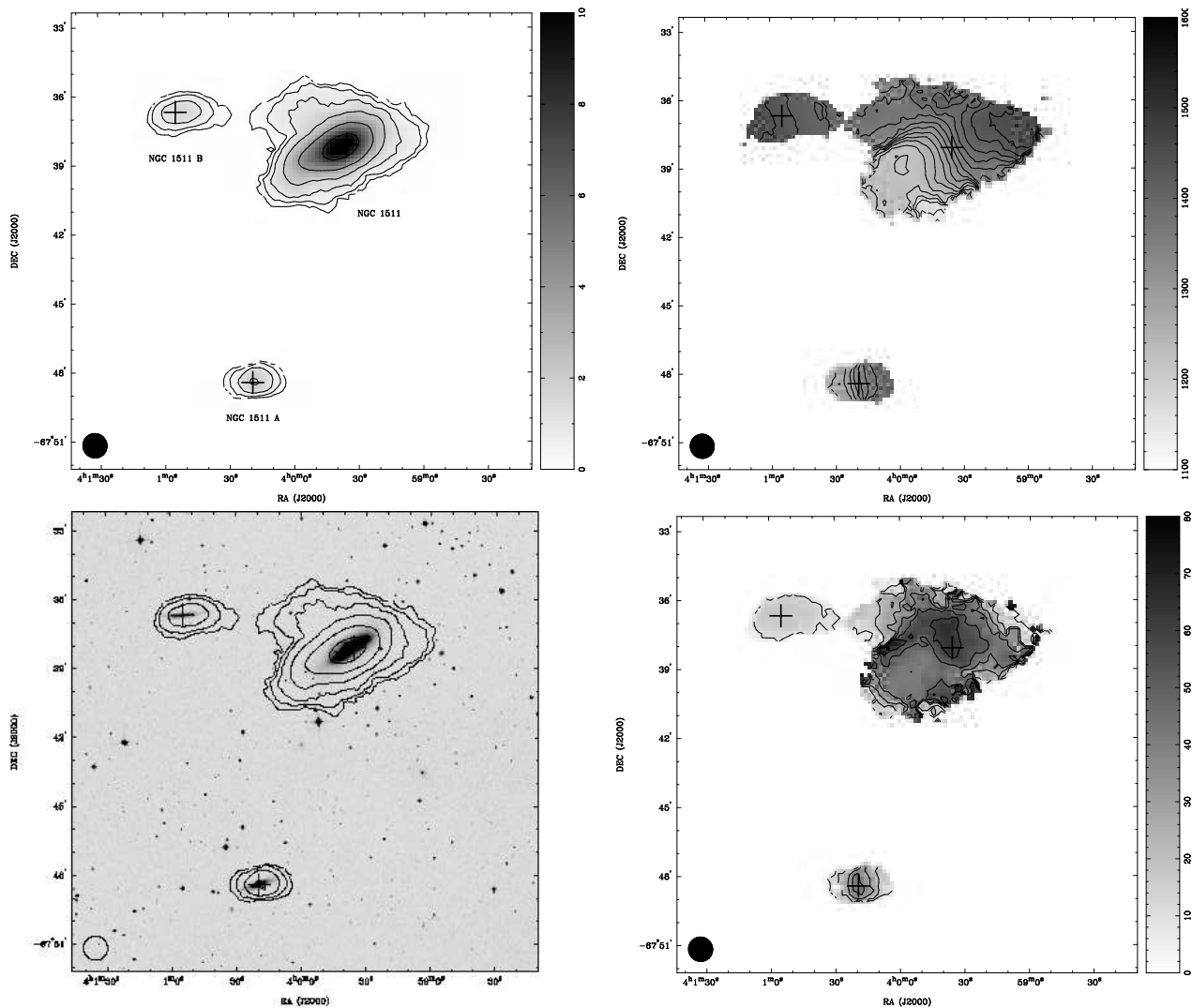


**Figure 4.** The H I gas dynamics of the galaxy group NGC 1511 (using ‘natural’ weighting). The optical galaxy centers (see Table 1) are marked. — **(top left)** H I distribution (0. moment). The contour levels are 0.25, 0.5, 1, 2, 4 and 8 Jy beam<sup>-1</sup> km s<sup>-1</sup> (corresponding to H I column densities of  $6.9 \times 10^{19}$  to  $2.2 \times 10^{21}$  atoms cm<sup>-2</sup>). — **(top right)** Mean H I velocity field (1. moment). The contour levels range from 1160 to 1480 km s<sup>-1</sup>, in steps of 20 km s<sup>-1</sup>. — **(bottom left)** H I distribution (contours) overlaid onto an optical image (greyscale) from the Digitised Sky Survey (DSS). The contour levels are as in (a). — **(bottom right)** H I velocity dispersion (2. moment). The contour levels are 10, 20, 30, 40, 50, and 60 km s<sup>-1</sup>. — The synthesized beam ( $64'' \times 63''$ ) is marked in the bottom left corner.

tle (if any) diffuse H I emission has been filtered out by the interferometric observation, i.e. the NGC 1511 group does not contain large amounts of un-detected H I gas. This is perhaps not surprising as the main interaction appears to occur between NGC 1511 and NGC 1511B and those scales are well covered by the ATCA observations.

Previous H I measurements of NGC 1511, obtained with the 64-m Parkes telescope, include  $F_{\text{HI}} = 63.7 \pm 6.1$  Jy km s<sup>-1</sup> (Reif et al. 1982), 85.3 Jy km s<sup>-1</sup> (Bajaja & Martin 1985), and 73.6 Jy km s<sup>-1</sup> (Mathewson & Ford 1996).

**Table 3.** H I properties of the galaxies and the bridge in the NGC 1511 group as measured with the ATCA.

Object	velocity range (km s <sup>-1</sup> )	$F_{\text{HI}}$ (Jy km s <sup>-1</sup> )	$M_{\text{HI}}$ ( $10^8 M_{\odot}$ )
group	1130–1510	74	53.5
NGC 1511	1130–1510	66.4	48.0
NGC 1511A	1240–1410	2.8	2.0
NGC 1511B	1370–1480	5.1	3.7

## 5 DISCUSSION

### 5.1 Signatures of Galaxy Interactions

Gaseous, intergalactic emission is detected between NGC 1511 and NGC 1511B in the velocity range from

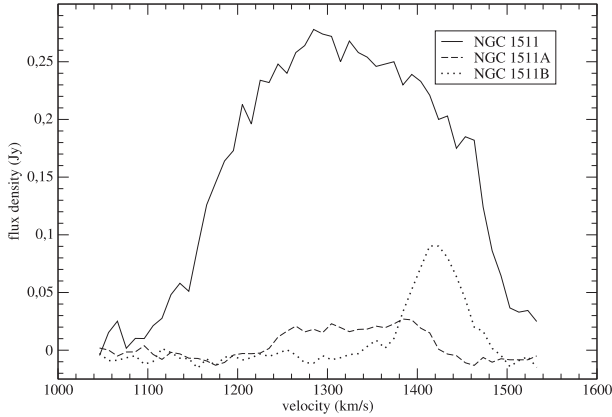


**Figure 3.** Integrated H I spectra of the three galaxies in the NGC 1511 group.

$\sim 1320$  to  $1430 \text{ km s}^{-1}$  (see Figs. 2 and 5). It commences at the north-western side of NGC 1511 and appears to curve around to the western side of NGC 1511B, extending over a distance of at least 37 kpc. The overall bridge area contains up to  $\sim 6 \text{ Jy km s}^{-1}$ , corresponding to an H I mass of  $\sim 4 \times 10^8 M_{\odot}$ ; this gas is currently attributed to either NGC 1511 or NGC 1511B in Table 3 because, with the current data, it is impossible to exactly specify how much H I gas lies between the galaxies. No stellar counterpart to the bridge has been detected in the available optical sky surveys.

The stellar distribution of NGC 1511B is extremely thin and edge-on. Its main body extends  $1'.7$  (9 kpc) along the major axis. In addition, we find a faint extension towards the west with a prominent H II region at its tip which corresponds to the H I maximum in the  $1393 \text{ km s}^{-1}$  channel map. The H I and the stellar disk of NGC 1511B seem to be elongated and severely distorted, especially in the direction of NGC 1511. In addition, the H I velocity field of NGC 1511B does not look like that of a normal rotating spiral galaxy. The iso-velocity contours are inclined with respect to the disk major-axis, at an angle of  $\sim 45^{\circ}$ , and are generally irregular (see Fig. 8). The velocity dispersion stays around  $17 \text{ km s}^{-1}$  throughout the disk. It seems that the H I gas distribution of NGC 1511B has been distorted and partially stripped off by gravitational forces during the interaction/collision with its massive neighbour, NGC 1511. The dynamical mass estimate given for NGC 1511B (see Table 4) is highly uncertain as the actual rotational velocity of the galaxy is unknown.

Another most interesting feature found near NGC 1511 is a *peculiar vertical ridge* ( $\sim 1'.5$  in length) only visible in deep optical images. It is located  $\sim 3'$  east of the centre of NGC 1511 and corresponds to a distinct region in the H I velocity field of NGC 1511 (see Fig. 7). While this region is peculiar with respect to the rotation of NGC 1511, it shows remarkably regular iso-velocity contours perpendicular to the ridge. We tentatively conclude that what appears like a peculiar ridge actually is the stellar remnant of a tidally-disrupted galaxy in the NGC 1511 group.

Bridges between galaxies, either consisting of gas only or with a stellar component, are observed in several galaxy pairs (e.g., Irwin 1994; Smith, Struck & Pogge 1997; Struck & Smith 2003; Koribalski & Dickey 2004). Simulations show

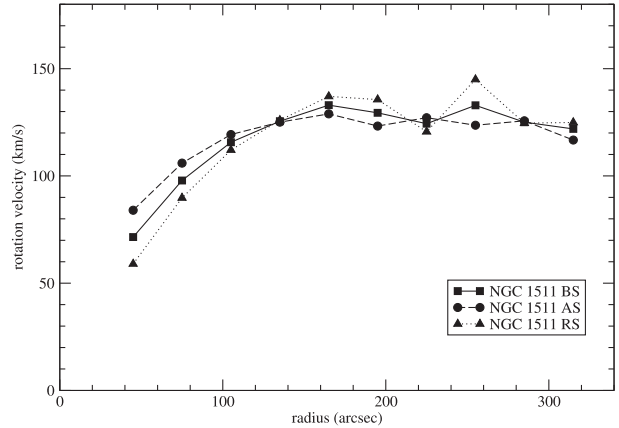


**Figure 6.** Rotation curve model for NGC 1511 for the approaching, receding and both sides. For a description of the fit parameters and their uncertainties see Section 5.2.

two different mechanisms for developing bridges. Toomre & Toomre (1972) first predicted bridges to be formed by tidal forces. This process is successfully modeled by Barnes & Hernquist (1991) and Mihos & Hernquist (1996), considering an impact parameter larger than the disk radius. In this case stars and gas are stripped out in the bridge. Struck (1997) discusses the formation of “splash” bridges which are formed during a close encounter (impact parameter smaller than disk radius). Gas clouds of both galaxies collide and form a gas bridge between them, typically without any stellar counterpart. In this kind of bridge no star formation is initially expected. The H I bridge between NGC 1511 and NGC 1511B seems to be a “splash” bridge, suggesting that NGC 1511B has plunged through the outer disk of NGC 1511 during its closest encounter.

## 5.2 The kinematics of NGC 1511 and its companions

In the inner part of its disk NGC 1511 shows a clear rotation pattern. By fitting all rotational parameters simultaneously for radii from  $30''$  to  $300''$  we find the kinematic center at  $\alpha, \delta(\text{J2000}) = 03^{\text{h}} 59^{\text{m}} 39^{\text{s}}.0 - 67^{\circ} 38' 10''.0$ , a systemic velocity of  $v_{\text{sys}} = 1333 \pm 5 \text{ km s}^{-1}$  and a position angle of  $PA = 300^{\circ} \pm 2^{\circ}$ . We note that there is a substantial offset between the optical center of NGC 1511 as given in Table 1, the 2MASS position, and the kinematic center as determined here. Since the fit of the position angle appeared constant with radius, we fixed its value to  $300^{\circ}$ . The inclination angle was difficult to fit, and we used  $i = 74^{\circ}$  (Table 1). With the two orientation parameters fixed, we derive a rotation curve for the approaching side (AS), the receding side (RS), and for both sides (BS) of NGC 1511 (see Fig. 6). While the approaching side of the galaxy shows a rather flat rotation curve, the receding side appears slightly irregular, possibly showing the effects of interactions which are most evident at the higher H I velocities in the system. Given a maximum H I rotation velocity of  $\sim 130 \text{ km s}^{-1}$  and an H I extent of  $\sim 300''$  (25 kpc) we derive a dynamical mass of  $\sim 10^{11} M_{\odot}$ . Due to the low angular resolution of our H I data compared to the size of the two companion galaxies, we were not able to fit their rotation curves.

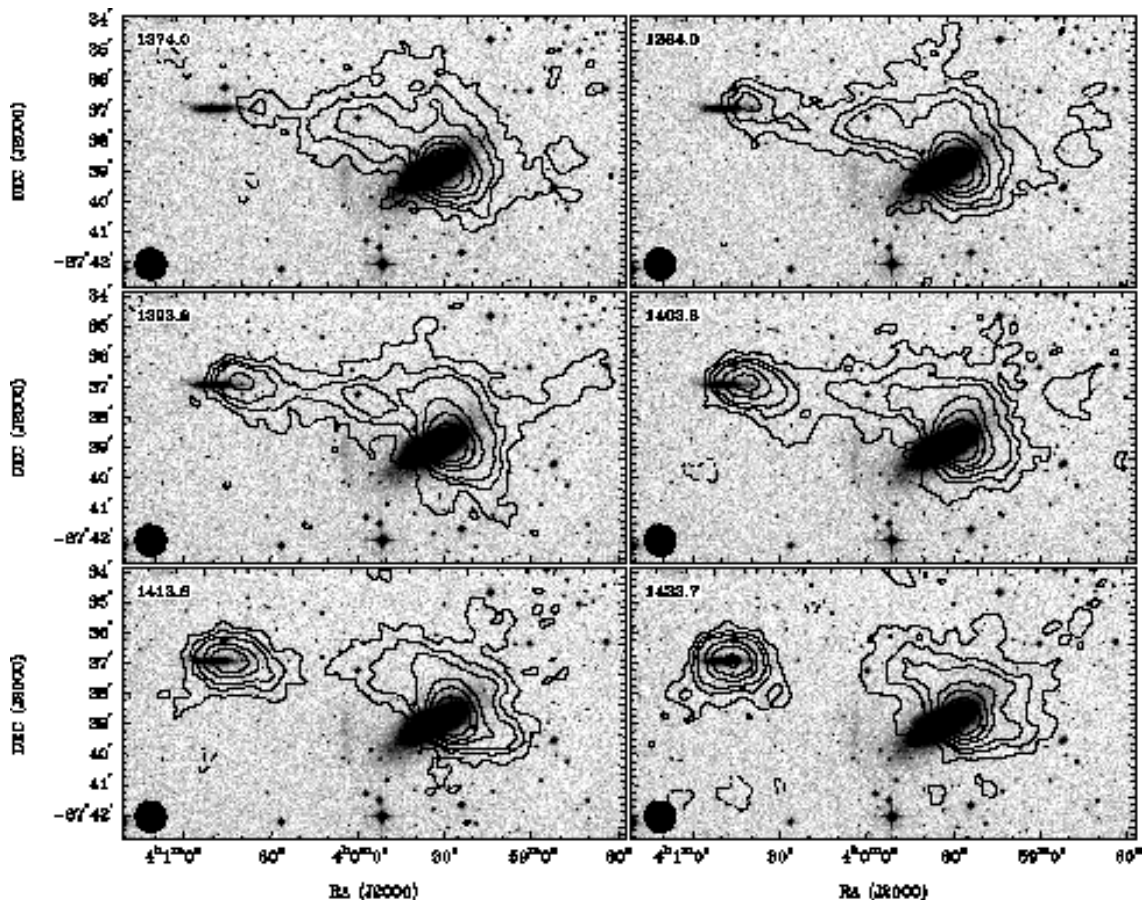


**Figure 5.** HI channel maps (from 1374 to 1424  $\text{km s}^{-1}$ ) overlaid onto a high contrast B-band image from the Supercosmos sky survey, emphasizing the narrow bridge between the interacting galaxies NGC 1511 and NGC 1511B. The contour levels are  $-3, 3, 6, 9, 15, 21,$  and  $30 \text{ mJy beam}^{-1}$ . The beam is displayed at the bottom left corner and the heliocentric velocity of each channel at the top left.

In Table 4 we list the systemic velocities, the rotation velocities and the HI radii of all three galaxies in the NGC 1511 group, as well as their dynamical masses and mass-to-light ratios. For NGC 1511A and NGC 1511B we estimate  $v_{\text{sys}}$  as the central velocity of the HI spectrum and  $v_{\text{rot}}$  as the half width of each spectrum, corrected for inclination taken from Table 1.

Adding the dynamical masses of the three galaxies together results in  $M_{\text{tot}}(\text{group}) = 1.2 \times 10^{11} M_{\odot}$ . For comparison, the virial mass (see Heisler, Tremaine & Bahcall 1985) of the NGC 1511 group is  $\sim 4.4 \times 10^{11} M_{\odot}$ , a factor 3.7 larger.

The HI velocity field of NGC 1511 (Fig. 7) shows a broad distribution with an extension to the south-east towards the peculiar optical ridge. In that area the optical image of NGC 1511 also shows peculiarities such as outflows and diffuse extended emission.

## 6 CONCLUSIONS

ATCA HI and 20-cm radio continuum observations of the NGC 1511 triplet reveal an HI-rich group with a striking gaseous bridge between the massive galaxy NGC 1511 and its minor companion NGC 1511B as well as substantial star formation in the disk of NGC 1511. While the gas distribu-

tion of NGC 1511B is strongly affected by the interaction, a second, more distant companion galaxy, NGC 1511A, remains unaffected. There may have been a fourth member of the galaxy group which now appears to be completely disrupted, leaving only the faint stellar remnant and a merging HI distribution. In the following we briefly summarise our results:

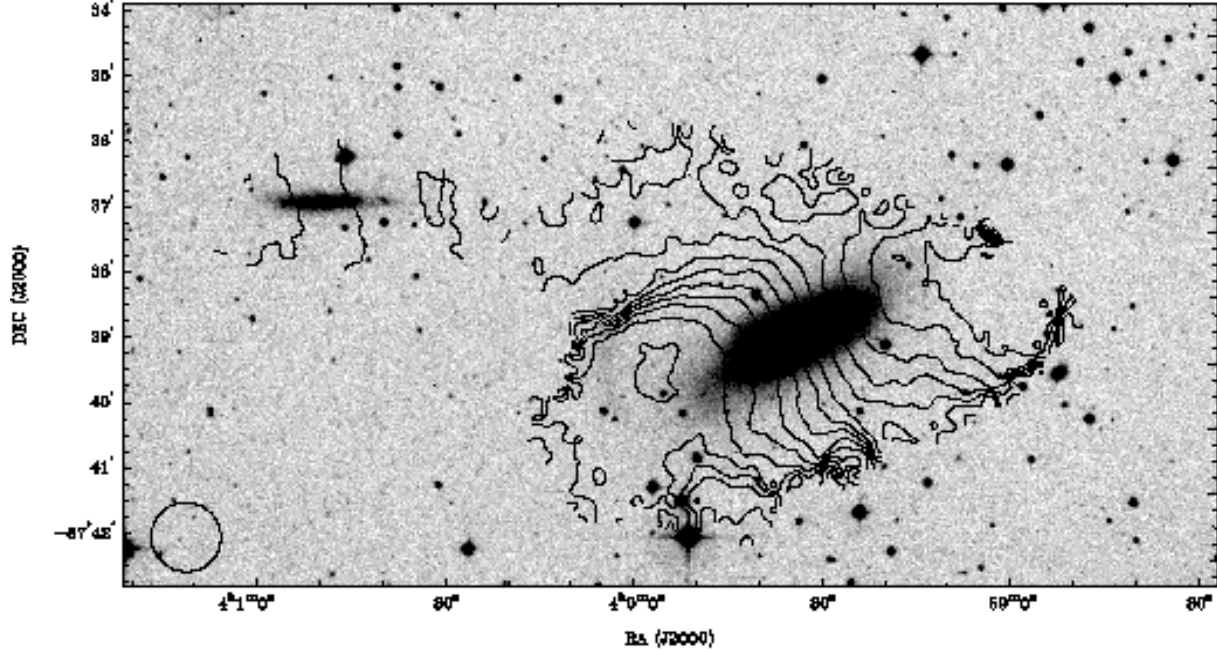
- HI emission was detected from all three galaxies in the NGC 1511 triplet. Assuming a distance of 17.5 Mpc for the group we derive HI masses of  $M_{\text{HI}} = 4.8 \times 10^9 M_{\odot}$  (NGC 1511),  $2.0 \times 10^8 M_{\odot}$  (NGC 1511A) and  $3.7 \times 10^8 M_{\odot}$  (NGC 1511B).

- In addition, we found an HI *bridge connecting NGC 1511 and NGC 1511B* with an HI mass of up to  $4 \times 10^8 M_{\odot}$ . The bridge, which was most likely formed through a close encounter of the two neighboring galaxies, has no apparent optical counterpart. The projected distance between NGC 1511 and NGC 1511B is  $\sim 37$  kpc, indicating an approximate time of  $\gtrsim 200$  Myr since their last collision.

- The HI distribution of NGC 1511B appears to have been severely stretched and displaced by the interaction/collision with NGC 1511. It has a rather narrow HI spectrum (for an edge-on galaxy) and an unusual HI velocity field. In contrast, the more distant companion, NGC 1511A, shows no signs of interaction.

**Table 4.** Derived properties of the galaxies in the NGC 1511 triplet.

Object	$v_{\text{sys}}$ ( $\text{km s}^{-1}$ )	$v_{\text{rot}}$ ( $\text{km s}^{-1}$ )	$r_{\text{HI}}$ (kpc)	$M_{\text{tot}}$ ( $10^9 M_{\odot}$ )	$M_{\text{HI}}/M_{\text{tot}}$	$M_{\text{tot}}/L_{\text{B}}$	$M_{\text{HI}}/L_{\text{B}}$
NGC 1511	1333	130	25	98	0.07	20	1.4
NGC 1511A	1325	88	8	14	0.02	20	0.4
NGC 1511B	1425	55?	10	7	0.07	23	1.7

**Figure 7.** Mean H I velocity field of the galaxy NGC 1511 (identical to Fig. 4) overlaid onto a B-band image from the SuperCOSMOS sky survey to emphasize the gas kinematics in the region of the peculiar optical ridge. The contour levels range from 1160 to 1480  $\text{km s}^{-1}$ , in steps of 20  $\text{km s}^{-1}$ .

- The *peculiar optical ridge* found to the east of NGC 1511 may be the stellar remnant of another group member, now completely disrupted by interactions with NGC 1511.

- For the NGC 1511 group we derive a total H I mass of  $5.4 \times 10^9 M_{\odot}$  ( $\sim 90\%$  of which resides in NGC 1511 itself), a combined dynamical mass of  $\sim 1.2 \times 10^{11} M_{\odot}$ , and a virial mass of  $\sim 4.4 \times 10^{11} M_{\odot}$ .

- High resolution ATCA radio continuum data show that most of the emission is occurring in the south-eastern part of the NGC 1511 disk, coincident with a prominent chain of H II regions. We measure a total 20-cm continuum flux density of 167 mJy for NGC 1511 which corresponds to a star formation rate (SFR) of  $7 M_{\odot} \text{ yr}^{-1}$ . Deriving the SFR from the FIR luminosity we determine a value of  $2.2 M_{\odot} \text{ yr}^{-1}$ , resulting in a  $q$  parameter of 2.34. For the companions, NGC 1511A and NGC 1511B, we derive upper limits of SFR =  $0.2 M_{\odot} \text{ yr}^{-1}$ .

#### ACKNOWLEDGMENTS

- We acknowledge use of the SuperCOSMOS Sky Survey.
- This research has made extensive use of the NASA/IPAC Extragalactic Database (NED) which is operated by the Jet Propulsion Laboratory, Caltech, under

contract with the National Aeronautics and Space Administration.

- The Digitized Sky Survey was produced by the Space Telescope Science Institute (STScI) and is based on photographic data from the UK Schmidt Telescope, the Royal Observatory Edinburgh, the UK Science and Engineering Research Council, and the Anglo-Australian Observatory.

- We thank the referee for some excellent comments.

#### REFERENCES

- Bajaja E., Martin C. 1985, AJ 90, 1783  
 Barnes J.E., Hernquist L. 1991, ApJ 370, L65  
 Broeils A.H., van Woerden H. 1994, A&AS 107, 129  
 Condon J.J. 1992, ARA&A 30, 575  
 Dahlem M., Lazendic J.S., Haynes R.F., Ehle M., Lisenfeld U. 2001, A&A 374, 42  
 Dahlem M., Ehle M., Jansen F., Heckman T.M., Weaver K.A., Strickland D.K. 2003, A&A 403, 547  
 Elfhag T., Booth R.S., Höglund B., Johansson L.E.B., Sandqvist Aa. 1996, A&AS 115, 439  
 Eskridge P.B. *et al.* 2000, ApJS 143, 73  
 Haarsma D.B., Partridge R.B., Windhorst R.A., Richards E.A. 2000, ApJ 544, 641  
 Heisler J., Tremaine S., Bahcall J.N. 1985, ApJ 298, 8



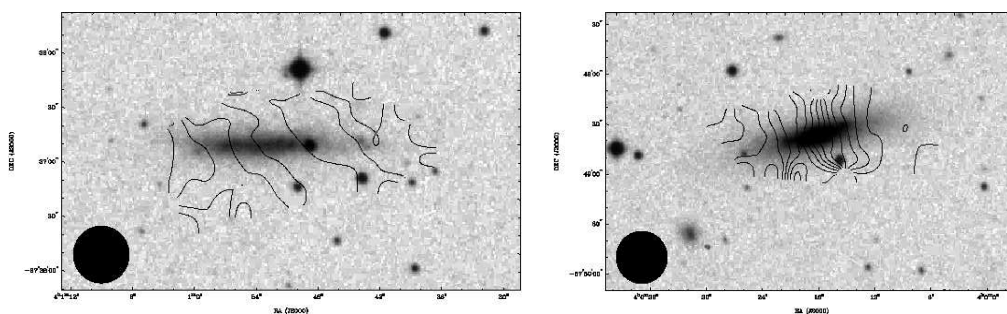


**Figure 8.** Mean H I velocity fields of the two companion galaxies, NGC 1511B (left) and NGC 1511A (right) overlaid onto B-band images from the SuperCOSMOS sky survey. For these images we used ‘robust’ weighting ( $r=0$ ), resulting in a synthesized beam of  $31.8'' \times 31.2''$ , to emphasize the inner disk. The contour levels range from 1400 to 1460  $\text{km s}^{-1}$  (for NGC 1511B) and 1250 to 1400  $\text{km s}^{-1}$  (for NGC 1511A), in steps of 10  $\text{km s}^{-1}$ . For comparison see Fig. 4.

- Helou G., Soifer B.T., Rowan-Robinson M. 1985, ApJ 298, L7  
 Hibbard J.E., van Gorkom J.H., Rupen M.P., Schiminovich D. 2001, in ‘Gas and Galaxy Evolution’, ASP Conf. Series Vol. 240, eds. J.E. Hibbard, M.P. Rupen, J.H. van Gorkom, p. 659  
 Huchtmeier W.K., Richter O.G. 1989, A General Catalog of H I Observations of Galaxies (Springer Verlag)  
 Huchtmeier W.K., Karachentsev I.D., & Karachentseva V.E. 2001, A&A 377, 801  
 Irwin, J.A. 1994, ApJ 429, 618  
 Jarrett T.H., Chester, T., Cutri, R., Schneider, S., Huchra, J.P. 2003, AJ 125, 525  
 Kennicutt R.C. 1998, ARA&A 36, 189  
 Kewley L.J. *et al.* 2000, ApJ 530, 704  
 Koribalski B., Dahlem, M., Mebold, U., Brinks, E. 1993, A&A 268, 14  
 Koribalski B. 1996, in “Barred Galaxies”, IAU Coll. 117, eds. Buta R., Crocker D.A., Elmegreen B.G., ASP Conf. Series Vol. 91, San Francisco, p. 172  
 Koribalski B. *et al.* 2004, AJ 128, 16  
 Koribalski B., Dickey, J.M. 2004, MNRAS 348, 1255  
 Lauberts A. 1982, ESO/Uppsala survey of the ESO(B) atlas  
 Lehnert M.D., Heckman T.M. 1995, ApJS 97, 89  
 Mathewson D.S., Ford V.L. 1996, ApJS 107, 97  
 Meyer, M.J., *et al.* 2004, MNRAS 350, 1195  
 Moshir M., *et al.* 1990, IRAS Faint Source Catalogue, version 2.0  
 Nordgren T.E., Chengalur J.N., Salpeter E.E., Terzian Y. 1997, AJ 114, 913  
 Mihos J.C., Hernquist L. 1996, ApJ 464, 641  
 Reif K., Mebold U., Goss W.M., van Woerden H., Siegman B. 1982, A&A 50, 451  
 Salpeter E.E., Hoffman G.L. 1996, ApJ 465, 595  
 Sandage A., Bedke J. 1994, The Carnegie Atlas of Galaxies  
 Sanders D.B., Egami E., Lipari S., Mirabel I.F., Soifer B.T. 1995, AJ 110, 1993  
 Schlegel D.J., Finkbeiner D.P., Davis M. 1998, ApJ 500, 525  
 Sekiguchi K., Wolstencroft R. 1993, MNRAS 263, 349  
 Smith B.J., Struck C., Pogge R.W. 1997, ApJ 483, 766  
 Strong A.W. *et al.* 1988, A&A 207, 1  
 Struck C. 1997, ApJS 113, 269  
 Struck C., Smith B.J. 2003, ApJ 589, 157  
 Thornley M.S., Schreiber N.M.F., Lutz D., Genzel R., Spoon H.W.W., Kunze D., Sternberg A. 2000, ApJ 539, 641  
 Toomre A., Toomre J. 1972, ApJ 178, 623  
 de Vaucouleurs G., de Vaucouleurs A., Corwin Jr. H.G., Buta R.J., Paturel G., Fouqué P. 1991, “Third Reference Catalogue of Bright Galaxies” (New York: Springer Verlag), [RC3]  
 Yun M.S., Ho P.T.P., Lo K.Y. 1994, Nature 372, 530